Supporting Information

for

Alkoxy-Substituted Anthra[1,2-*c*:5,6-*c*']bis([1,2,5]thiadiazole) (ATz): A New Electron-Acceptor Unit in the Semiconducting Polymers for Organic Electronics

Hiroki Mori[†], Shuhei Nishinaga[‡], Ryosuke Takahashi[‡], and Yasushi Nishihara[*,†]

[†]*Research Institute for Interdisciplinary Science, Okayama University, 3-1-1 Tsushimanaka, Kita-ku, Okayama 700-8530, Japan*

[‡]*Division of Earth, Life, and Molecular Sciences, Graduate School of Natural Science and Technology, Okayama University, 3-1-1 Tsushimanaka, Kita-ku, Okayama 700-8530, Japan.*

Phone: +81-86-251-7855

Fax: +81-86-251-7855

E-mail: ynishiha@okayama-u.ac.jp

1. *Copies of ¹H and ¹³C{¹H} NMR Charts and NOESY Spectra for the New Compounds*

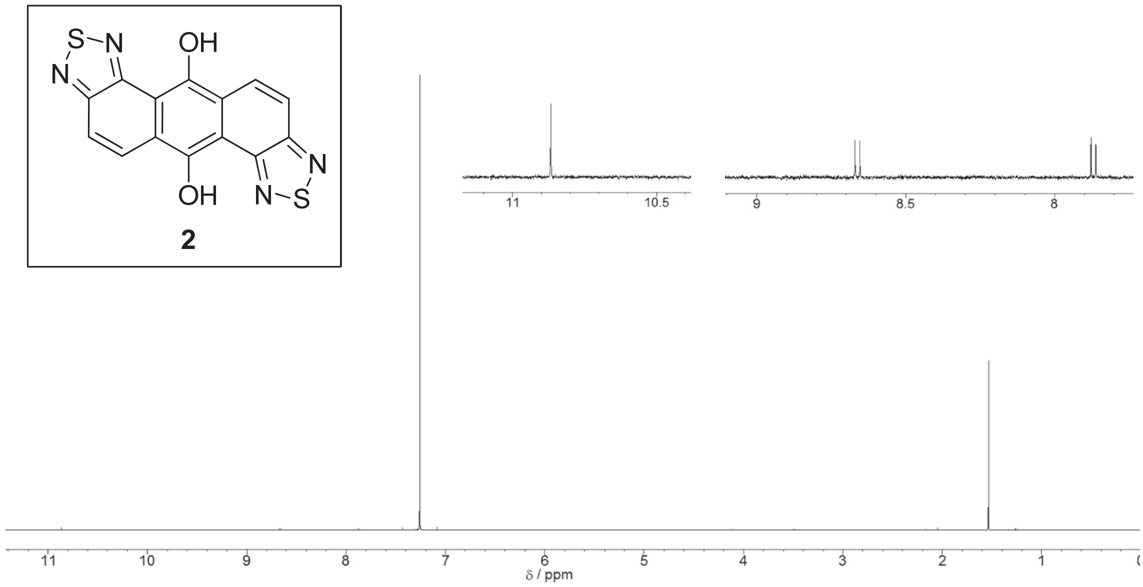

2

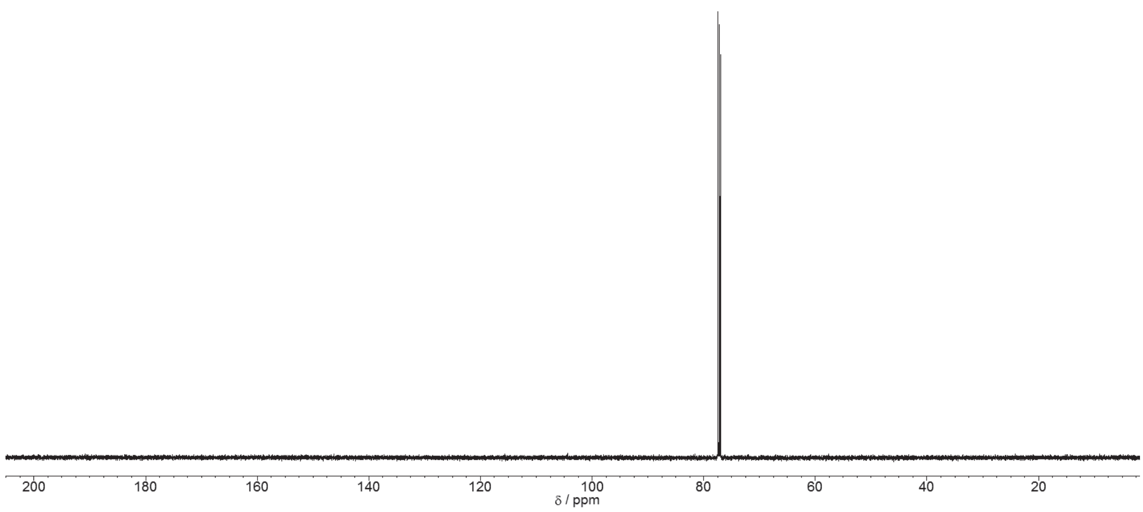

The ¹H and ¹³C{¹H} NMR spectra of **2** (in $CDCl_3$).

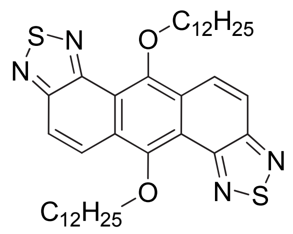

3a

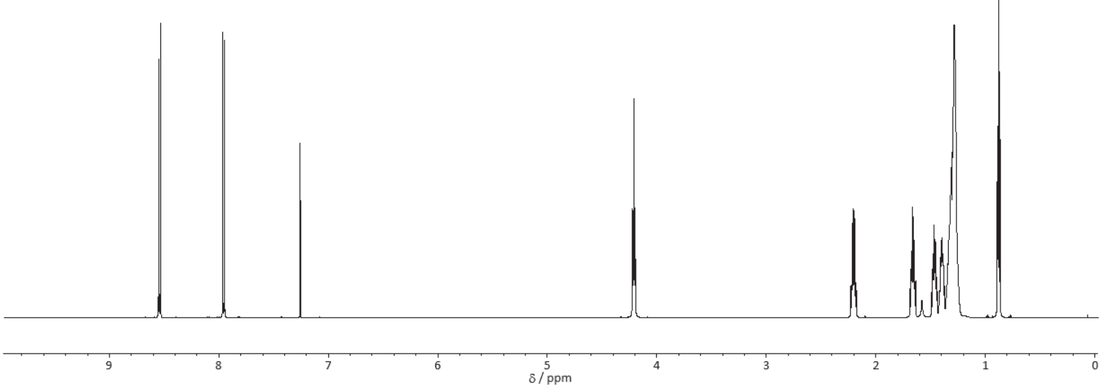

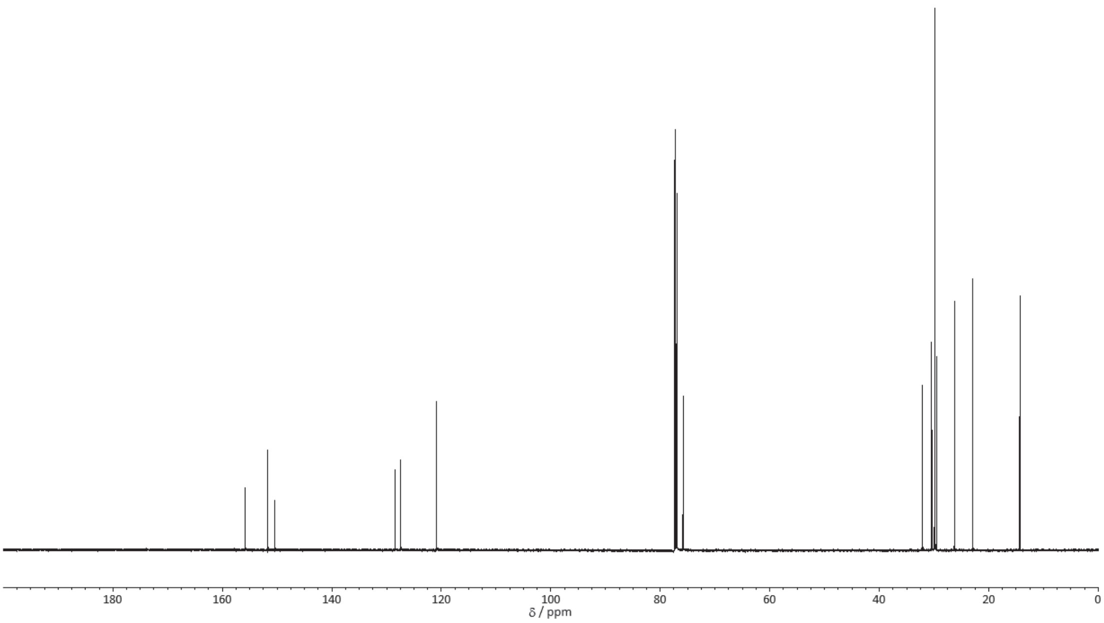

The ^{1}H and $^{13}C\{^{1}H\}$ NMR spectra of **3a** (in $CDCl_3$).

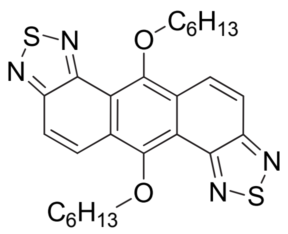

3b

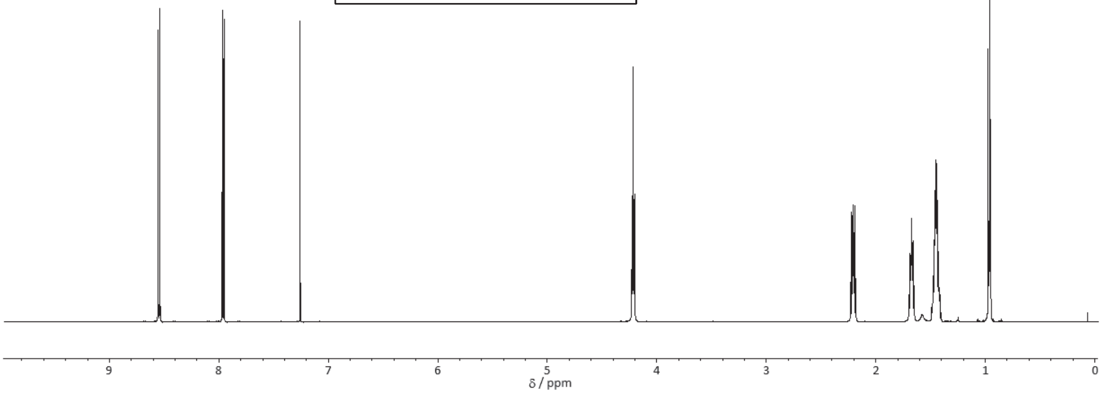

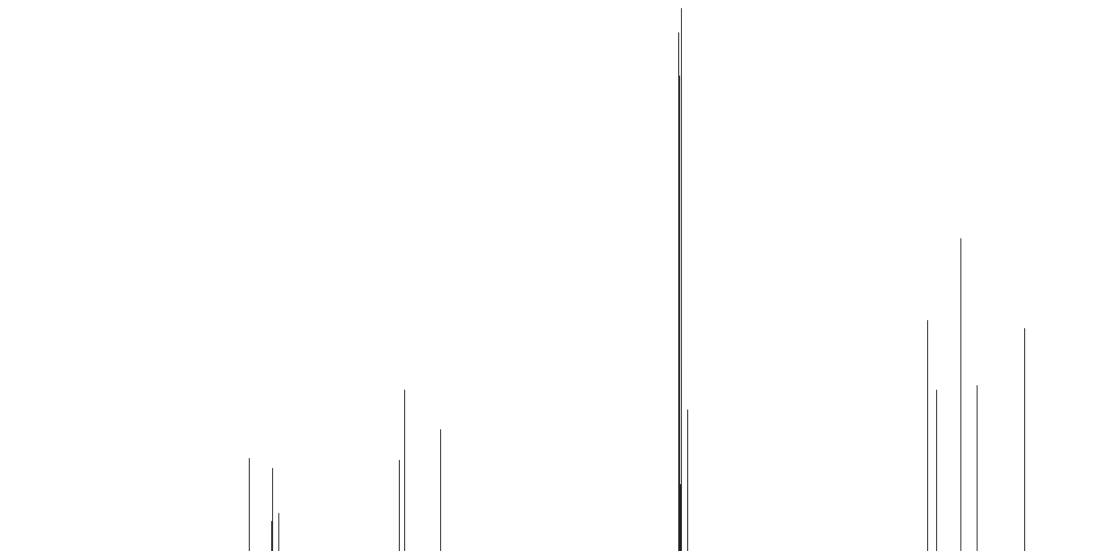

The ^{1}H and $^{13}C\{^{1}H\}$ NMR spectra of **3b** (in $CDCl_3$).

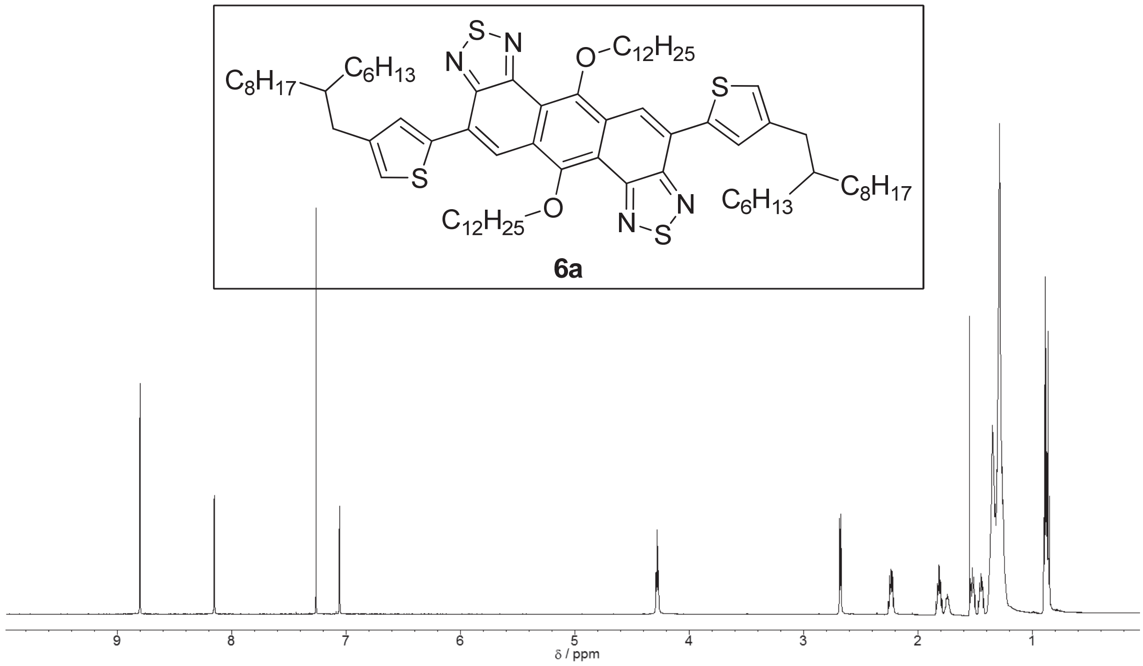

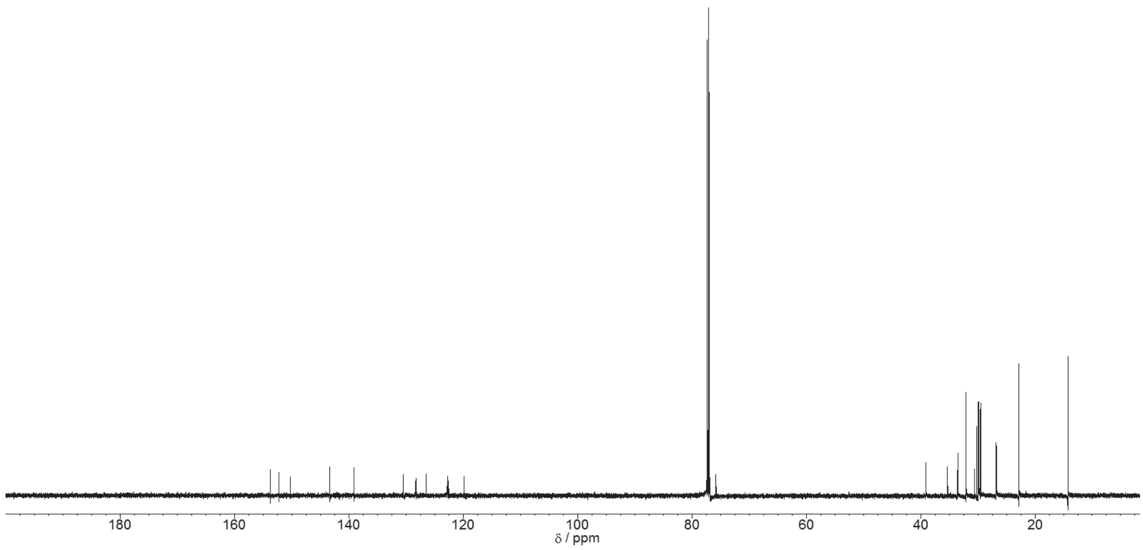

The ^{1}H and $^{13}C\{^{1}H\}$ NMR spectra of **6a** (in $CDCl_3$).

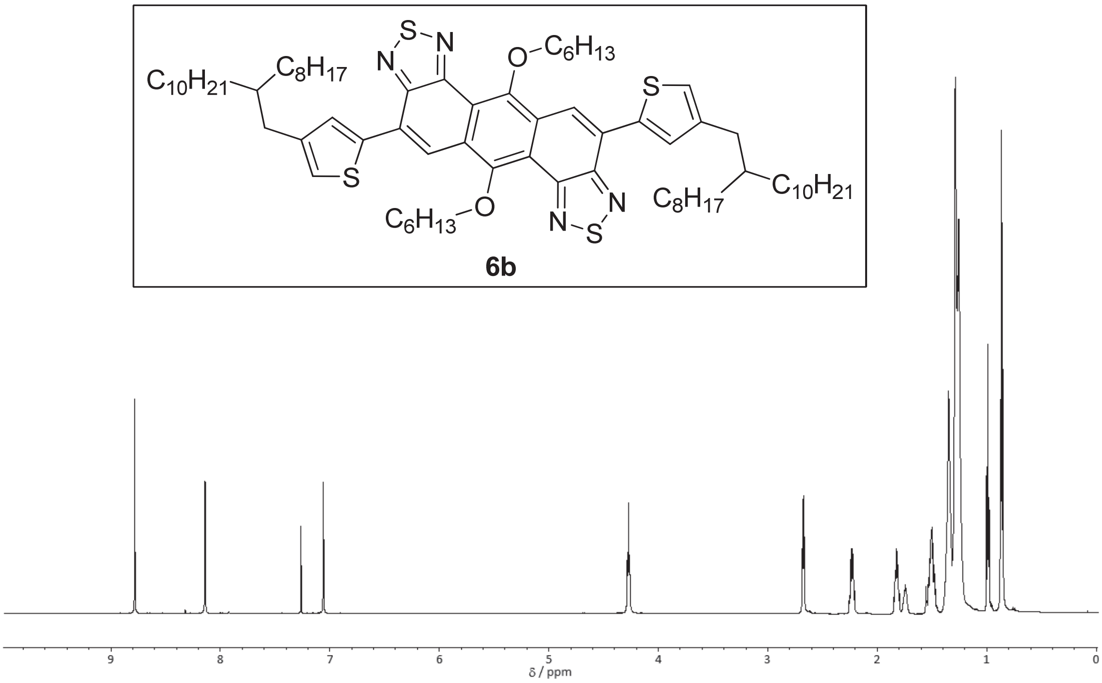

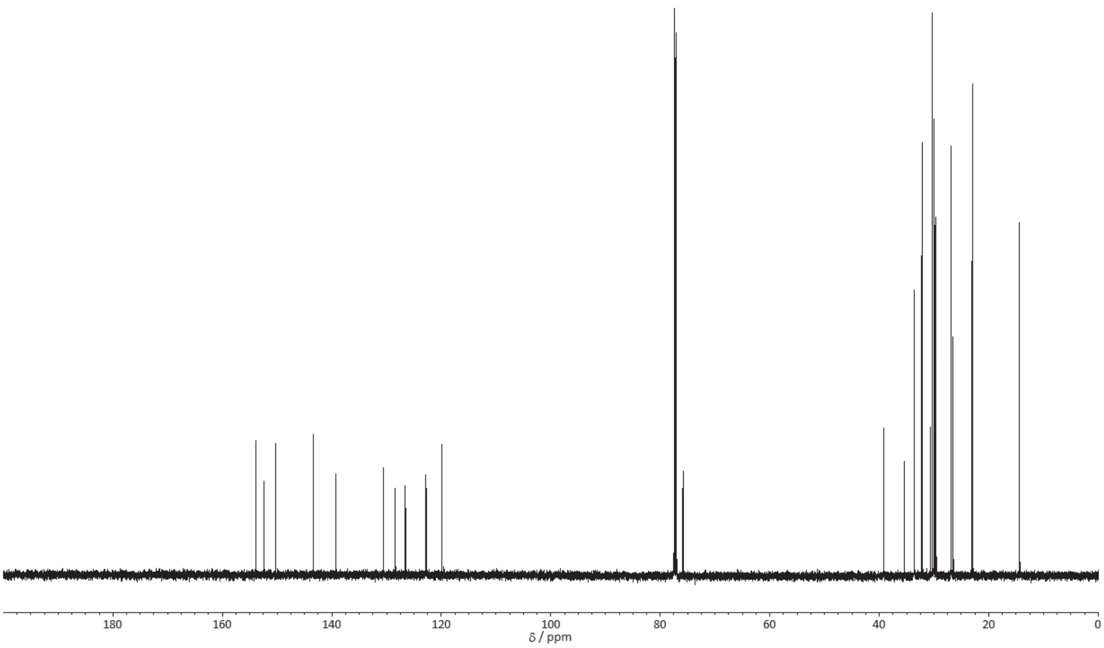

The ^{1}H and $^{13}C\{^{1}H\}$ NMR spectra of **6b** (in $CDCl_3$).

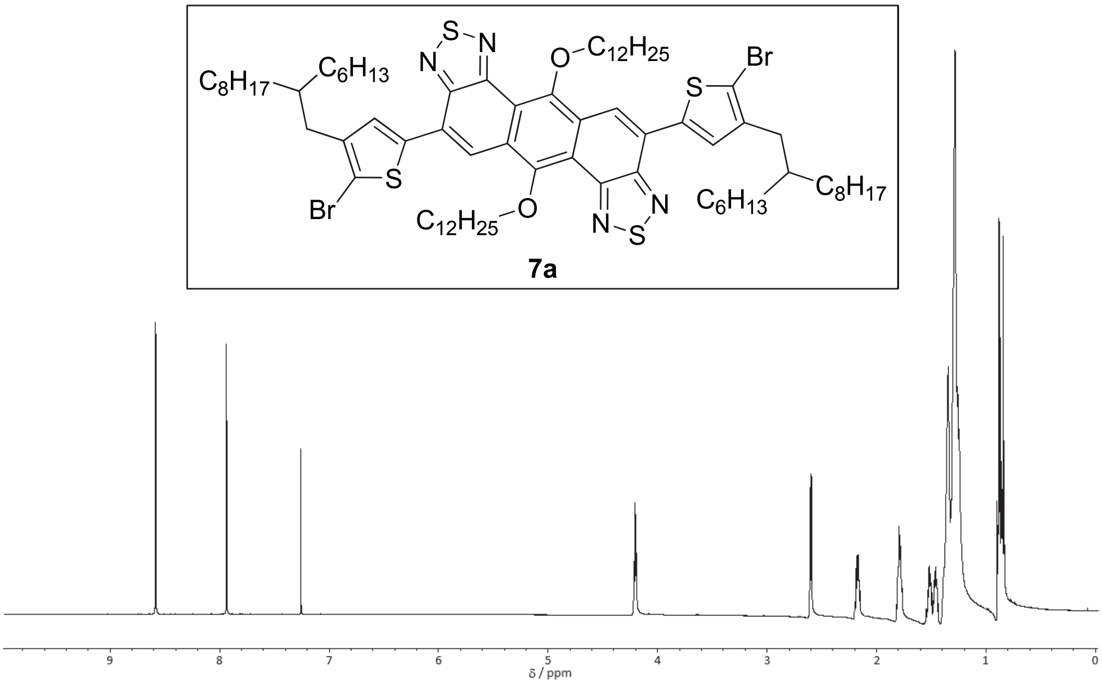

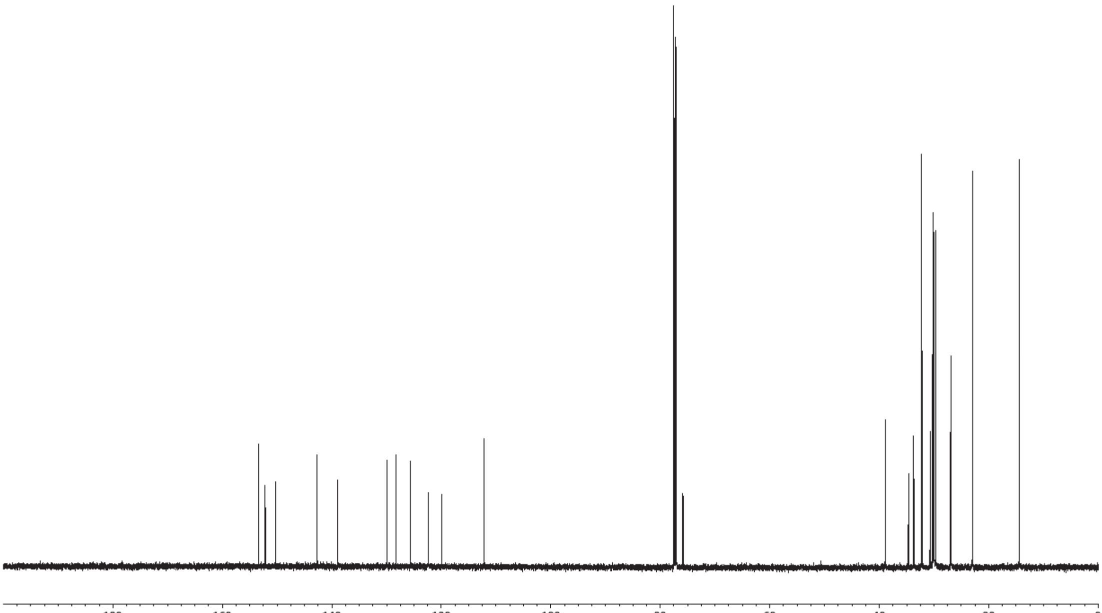

The ^{1}H and $^{13}C\{^{1}H\}$ NMR spectra of **7a** (in $CDCl_3$).

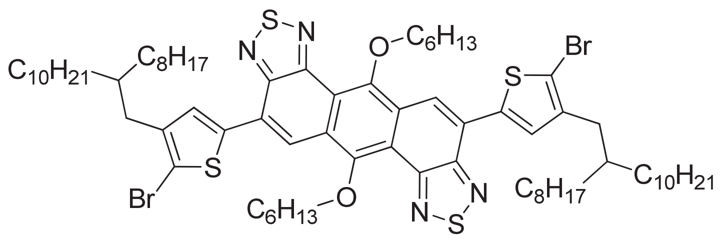

7b

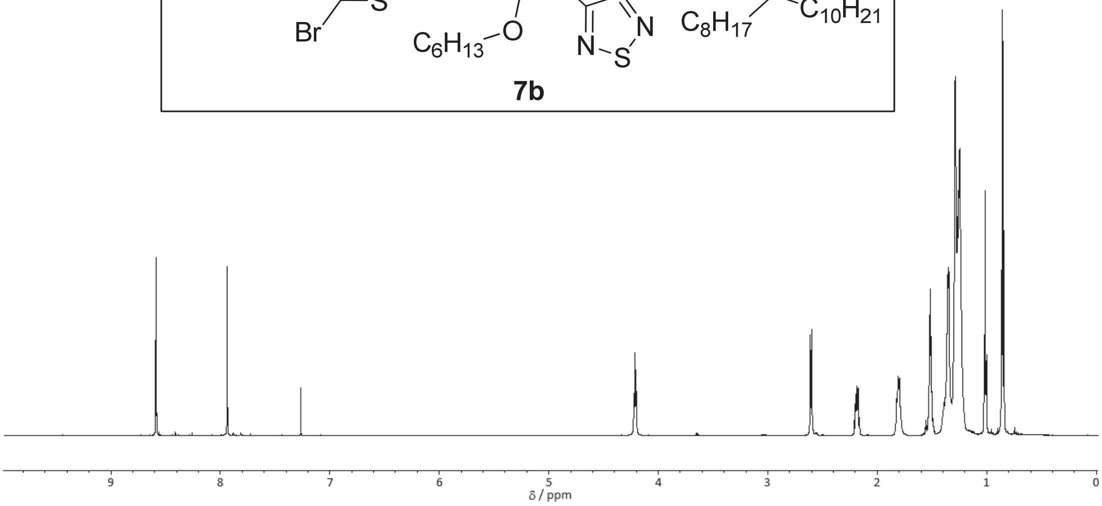

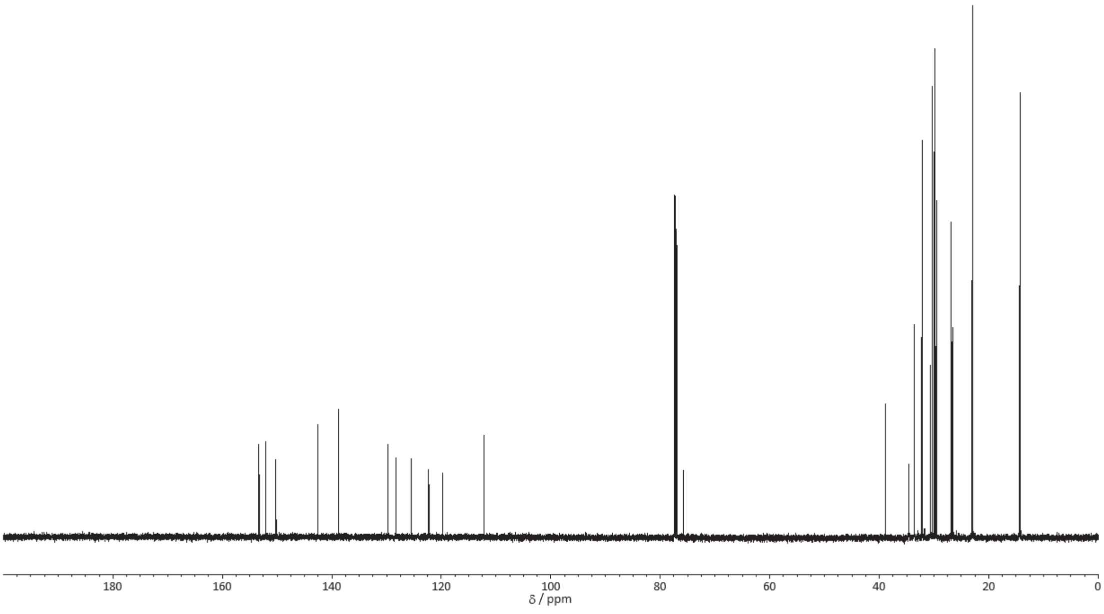

The ^{1}H and $^{13}C\{^{1}H\}$ NMR spectra of **7b** (in $CDCl_3$).

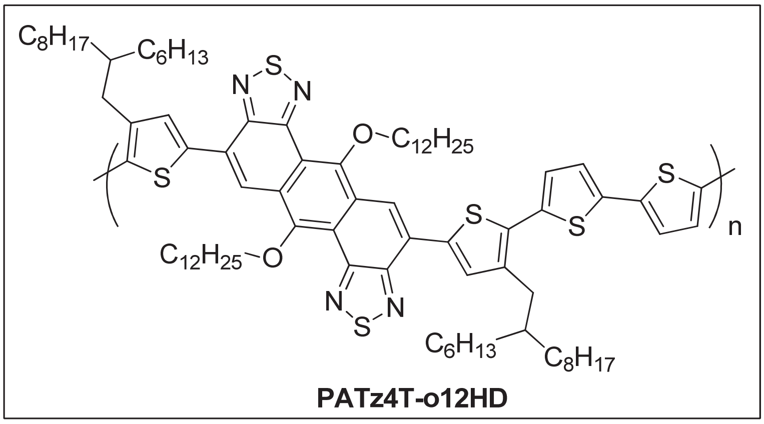

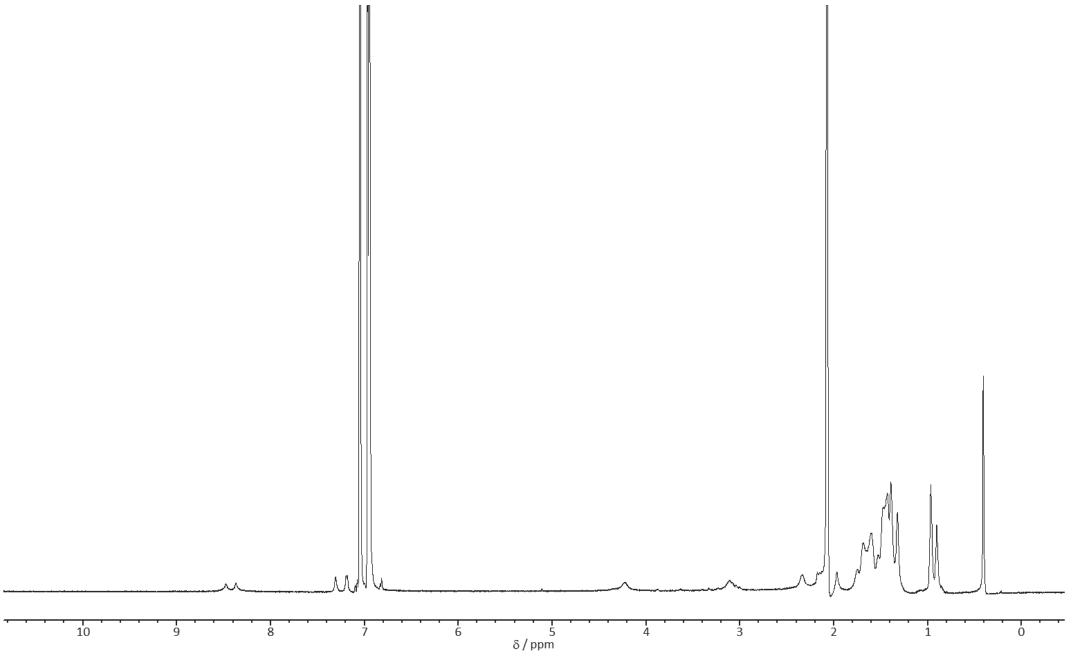

The [1]H NMR spectra of **PATz4T-o12HD** (in toluene-d_8, 80 °C).

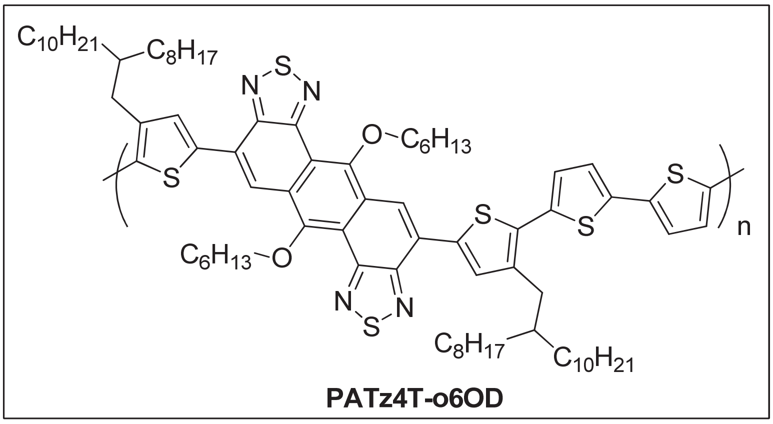

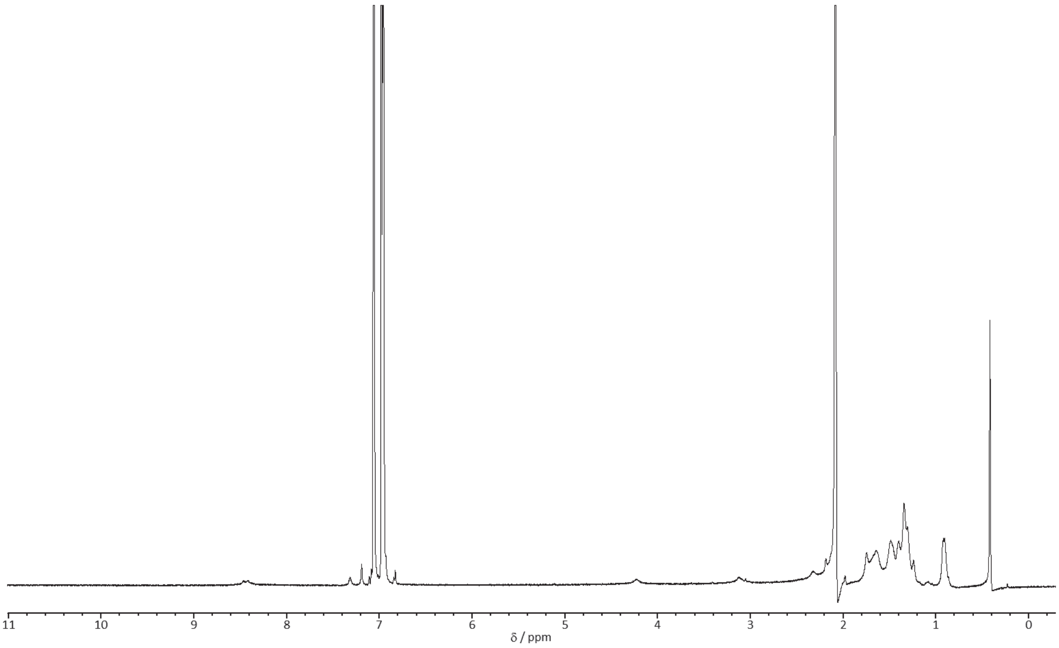

The [1]H NMR spectra of **PATz4T-o6OD** (in toluene-d_8, 80 °C).

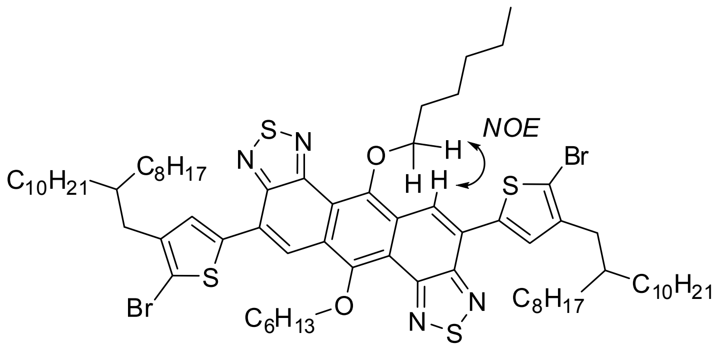
NOE
Br
S
N
O
H
C10H21
C8H17
C6H13

7b

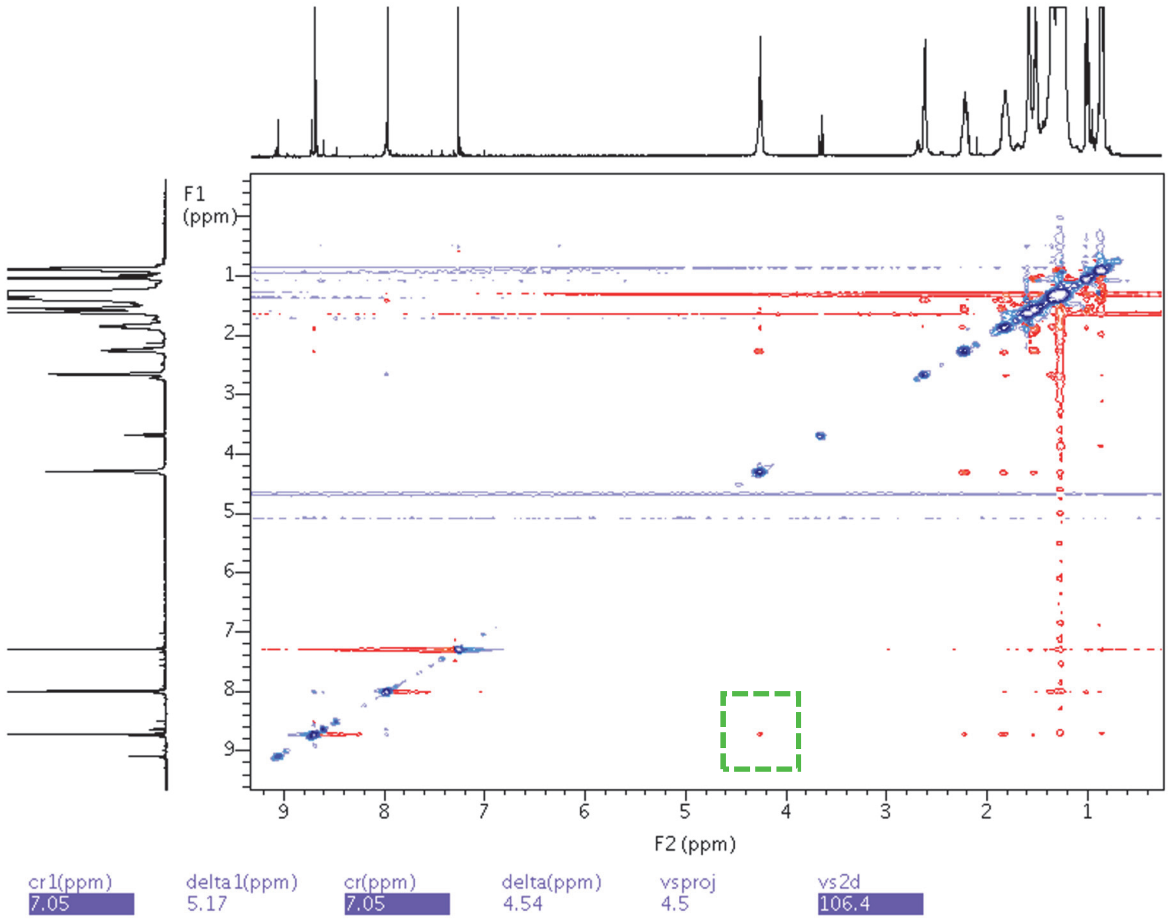
F1
(ppm)
F2 (ppm)
cr1(ppm)
7.05
delta1(ppm)
5.17
cr(ppm)
7.05
delta(ppm)
4.54
vsproj
4.5
vs2d
106.4

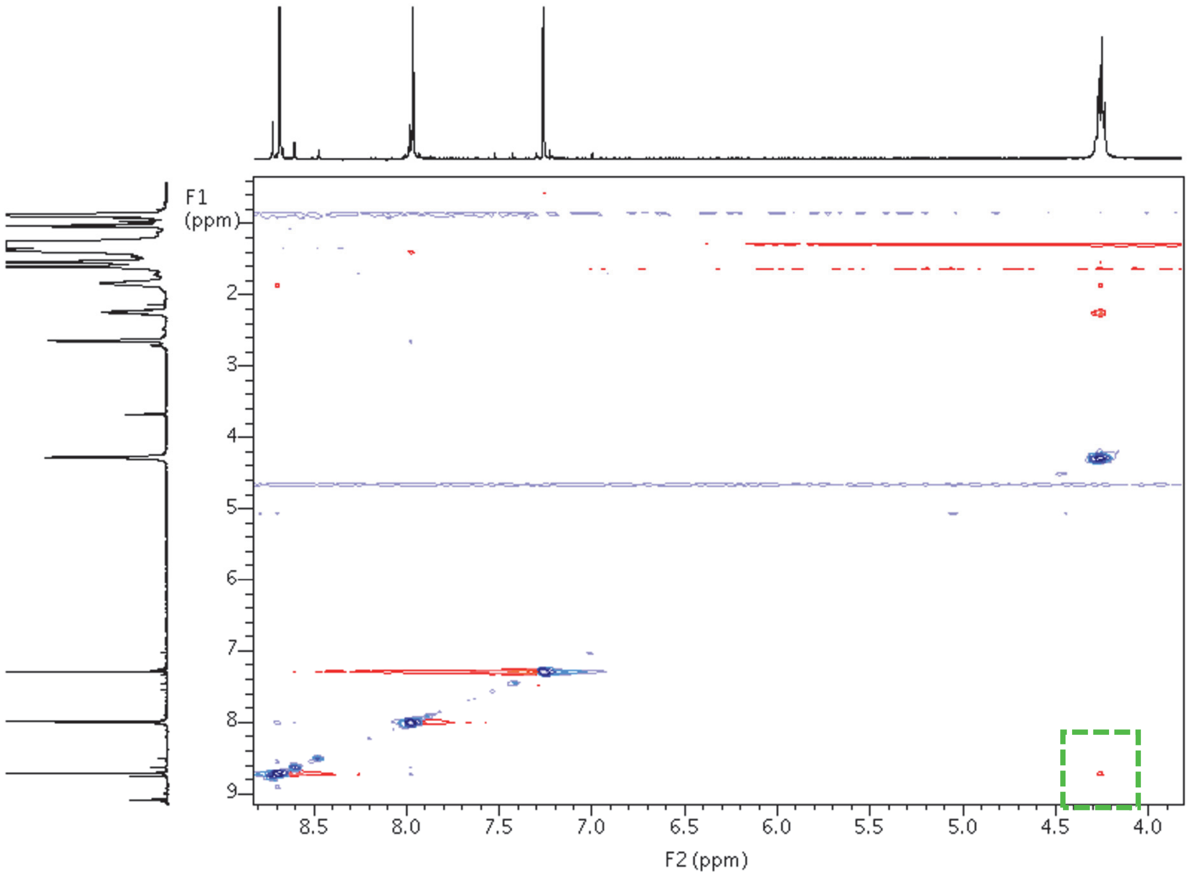

NOESY spectra of **7b** (in $CDCl_3$, rt).

2. DFT Calculations of Model Compound of PATz4T Polymers

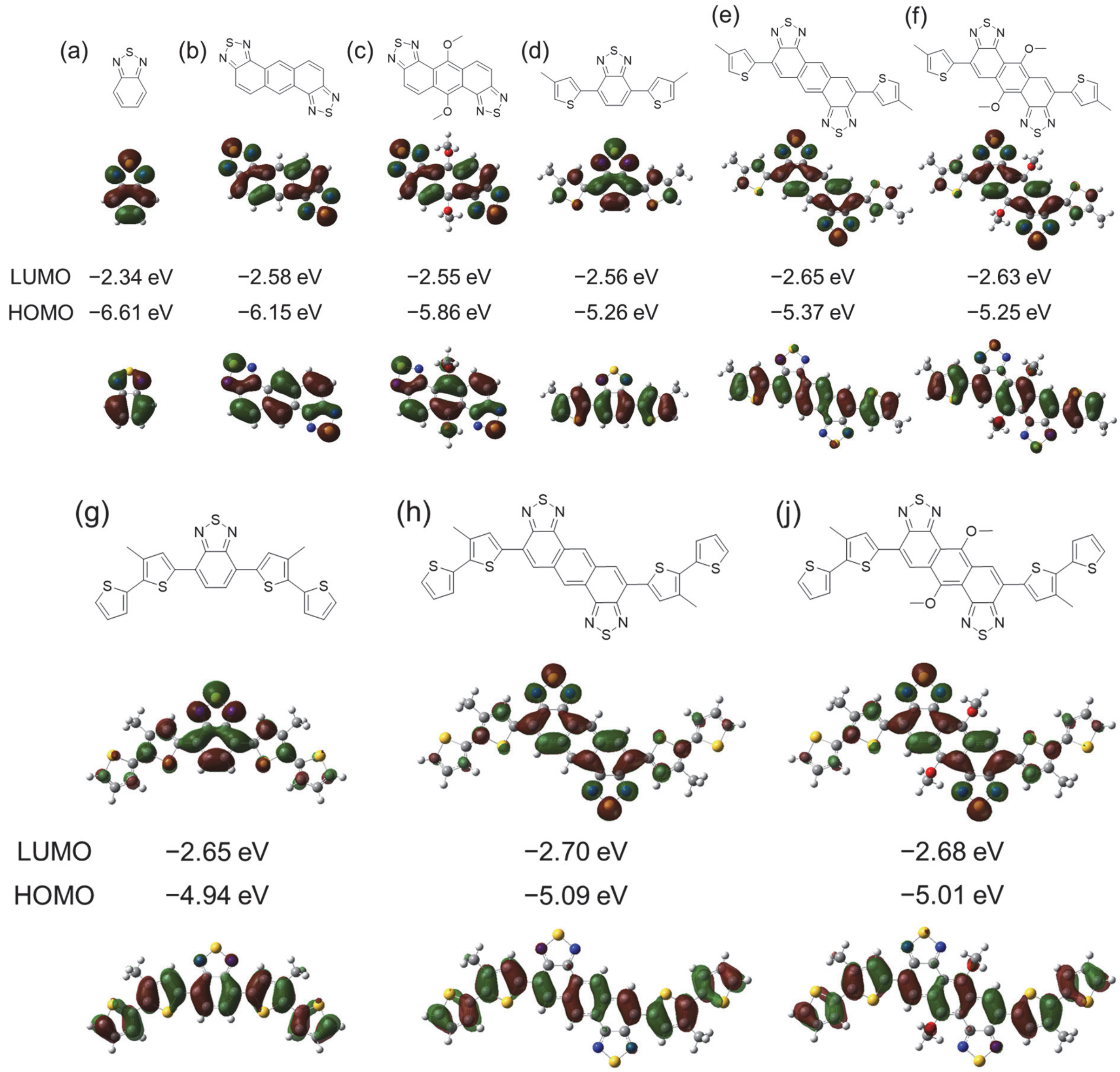

(j)

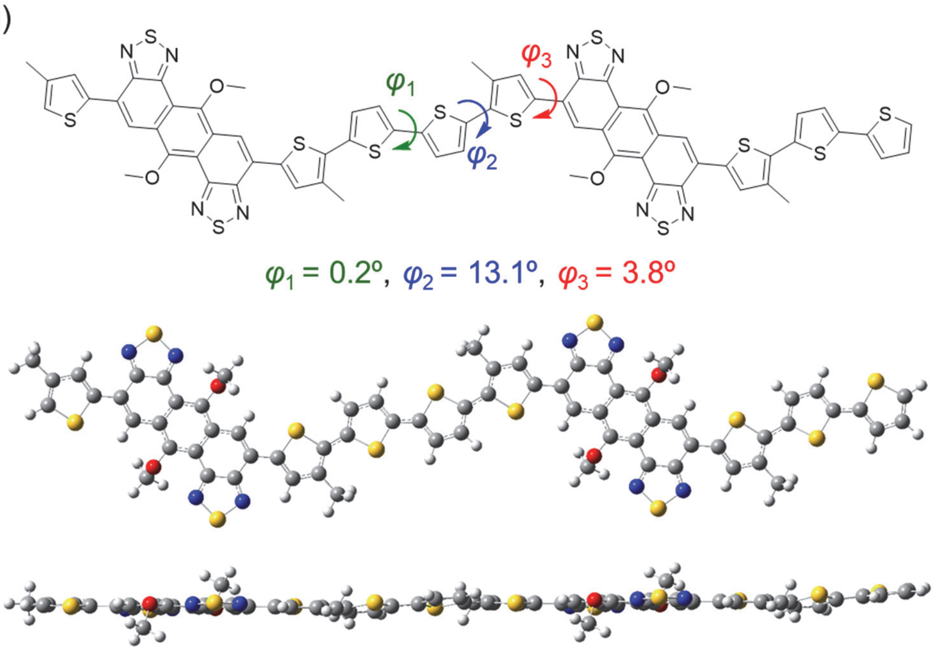

Figure S1. Geometry of HOMO and LUMO orbitals for (a) **BTz**, (b) **ATz**, (c) **ATzoMe**, (d) **BTz2T**, (e) **ATz2T**, (f) **ATz2ToMe**, (g) **BTz4T**, (h) **ATz4T**, and (i) **ATz4ToMe** calculated by using DFT at B3LYP/6-31G (d). (j) The optimized dimer structure of model compound for **PATz4T-oR^{1}R^2**. All alkyl groups are replaced with a methyl group for simplicity.

3. GPC Charts of PATz4T Polymers

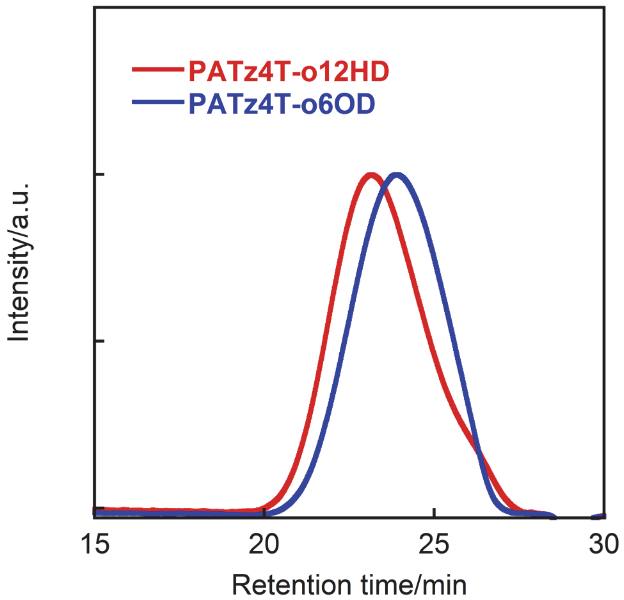

Figure S2. GPC Charts of **PATz4T** polymers.

4. Physicochemical Properties of BTz Derivatives

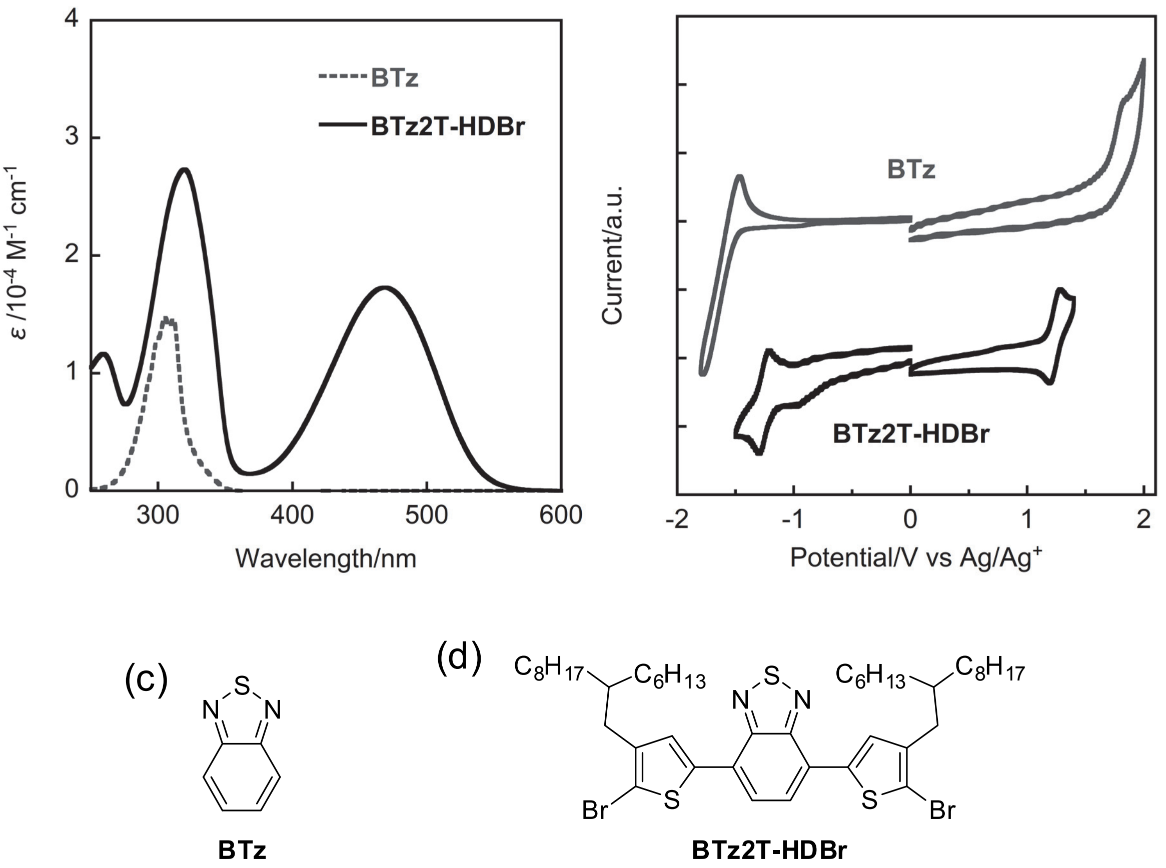

Figure S3. (a) UV-vis absorption spectra of BTz derivatives in CH_2Cl_2 solution and (b) cyclic voltammograms of BTz derivatives in CH_2Cl_2 solution with 0.1 M $TBAPF_6$ (Fc/Fc^+: $E_{1/2}$ = +0.44 V). Chemical structures of (c) parent BTz and (d) BTz2T-HDBr.

5. Output Curves and Optimization of PATz4T-Based OFETs

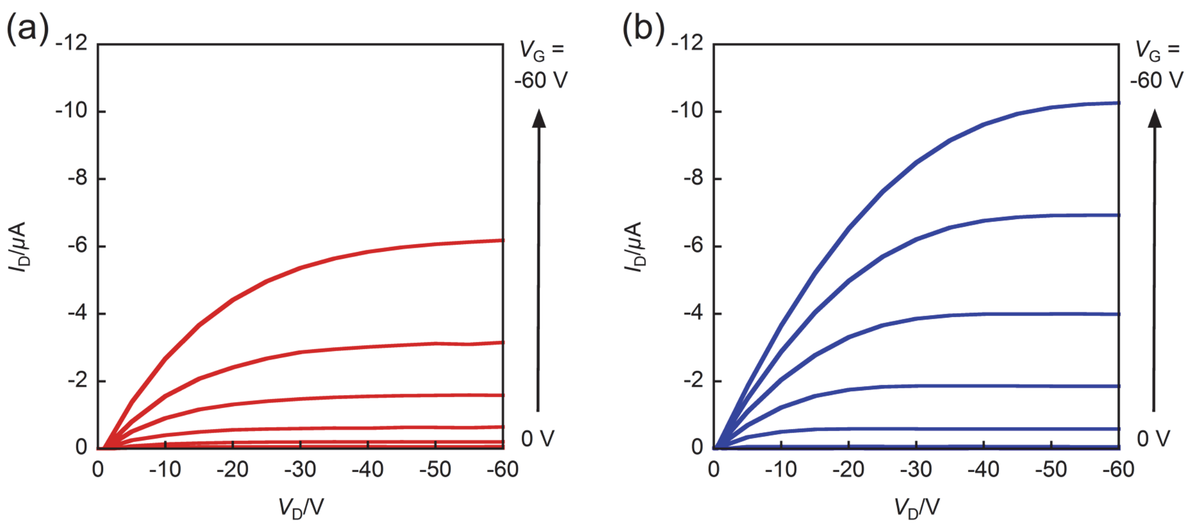

Figure S4. The output curves of (a) **PATz4T-o12HD-** and (b) **PATz4T-o6OD**-based OFET devices.

Table S1. OFET Performances of PATz4T-based Devices[a]

PATz4T	SAM[b]	T_{anneal}/°C[c]	μ_{FET}/cm^2 V^{-1} s^{-1} [d]	V_{th}/V	$I_{on/off}$
-o12HD	ODTS	–	2.74×10^{-4} (2.67×10^{-4})	+5 (+5)	10^4~10^6
	ODTS	200	4.59×10^{-4} (3.91×10^{-4})	−8 (−5)	10^1~10^2
	ODTS	250	1.18×10^{-3} (7.21×10^{-4})	−3 (+5)	10^1~10^4
	FOTS	250	0.025 (0.021)	−17 (−15)	10^3~10^4
-o6OD	ODTS	–	1.77×10^{-3} (1.36×10^{-3})	−8 (−2)	10^2~10^4
	ODTS	200	6.02×10^{-3} (4.44×10^{-3})	−11 (−8)	10^3~10^4
	ODTS	250	2.99×10^{-3} (2.23×10^{-3})	−8 (−2)	10^3~10^6
	FOTS	250	0.032 (0.023)	−11 (−6)	10^3~10^6

[a]Average values are shown in parentheses. [b]SAM = self-assembled monolayer. ODTS = *n*-octadecyltriethoxysilane. FOTS = 1*H*,1*H*,2*H*,2*H*-perfluorooctyltriethoxysilane. [c]Thermal annealing temperature. [d]Extracted from transfer curves in saturation regime.

6. Photovoltaic Properties of PATz4T-Based OPVs

Table S2. Solar Cell Performances of Polymer/$PC_{61}BM$-based Devices

PATz4T	p/n ratio[a]	solvent[b]	J_{sc}/mA cm^{-2}	V_{oc}/V	*FF*	PCE_{max} (PCE_{avg})/%
-o12HD	1:1	DCB	5.77	0.84	0.55	2.64 (2.07)
	1:2	DCB	2.99	0.86	0.46	1.19 (1.14)
	1:1	DCB+1 vol% DIO	6.02	0.82	0.56	2.76 (2.58)
	1:1	DCB+2 vol% DIO	5.95	0.81	0.71	3.44 (3.34)
	1:1	CB+1 vol% DIO	7.51	0.80	0.46	2.75 (2.12)
	1:1	CB+1 vol% DIH	6.22	0.81	0.72	3.63 (3.14)
	1:1	DCB+ 1 vol% DIH	6.39	0.82	0.73	3.81 (3.52)
-o6OD	1:1	CB	9.53	0.84	0.67	5.36 (5.04)
	1:2	CB	10.67	0.83	0.64	5.66 (5.42)
	1:2	DCB	9.24	0.83	0.71	5.42 (5.17)
	1:3	DCB	11.03	0.82	0.57	5.20 (5.10)
	1:2	CB+1 vol% DIO	10.48	0.80	0.52	4.31 (4.14)
	1:2	CB+1 vol% DPE	10.75	0.79	0.48	4.10 (3.90)
	1:2	CB+1 vol% CN	9.55	0.83	0.56	4.40 (4.29)

[a]Weight ratios of polymers and $PC_{61}BM$. [b]CB = chlorobenzene. DCB = *o*-dichlorobenzene. DIO = 1,8-diiodooctane. DPE = diphenyl ether. DIH = 1,6-diiodohexane. CN = 1-chloronaphthalene.

7. SCLC Hole Mobility of PATz4T-Based Hole-Only Devices

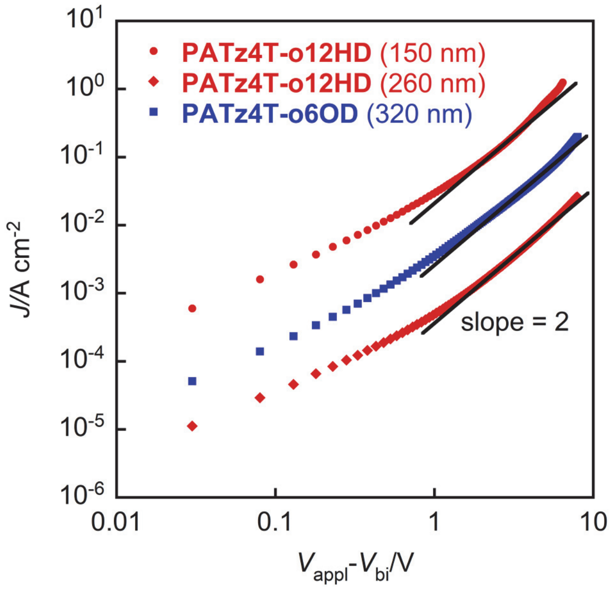

Figure S5. *J-V* characteristics of **PATz4T**-based hole-only devices with configuration of ITO/(PEDOT:PSS)/(polymer:$PC_{61}BM$)/MoO_3/Al. Blend ratios of polymer and $PC_{61}BM$ are 1:1 for **PATz4T-o12HD** and 1:2 for **PATz4T-o6OD**. The thickness of active layer is 150 nm or 260 nm for **PATz4T-o12HD**, and 320 nm for **PATz4T-o6OD**. No SCLC region was observed in **PATz4T-o6OD-**based hole-only devices due to its high current density.

7. AFM Images of PATz4T films

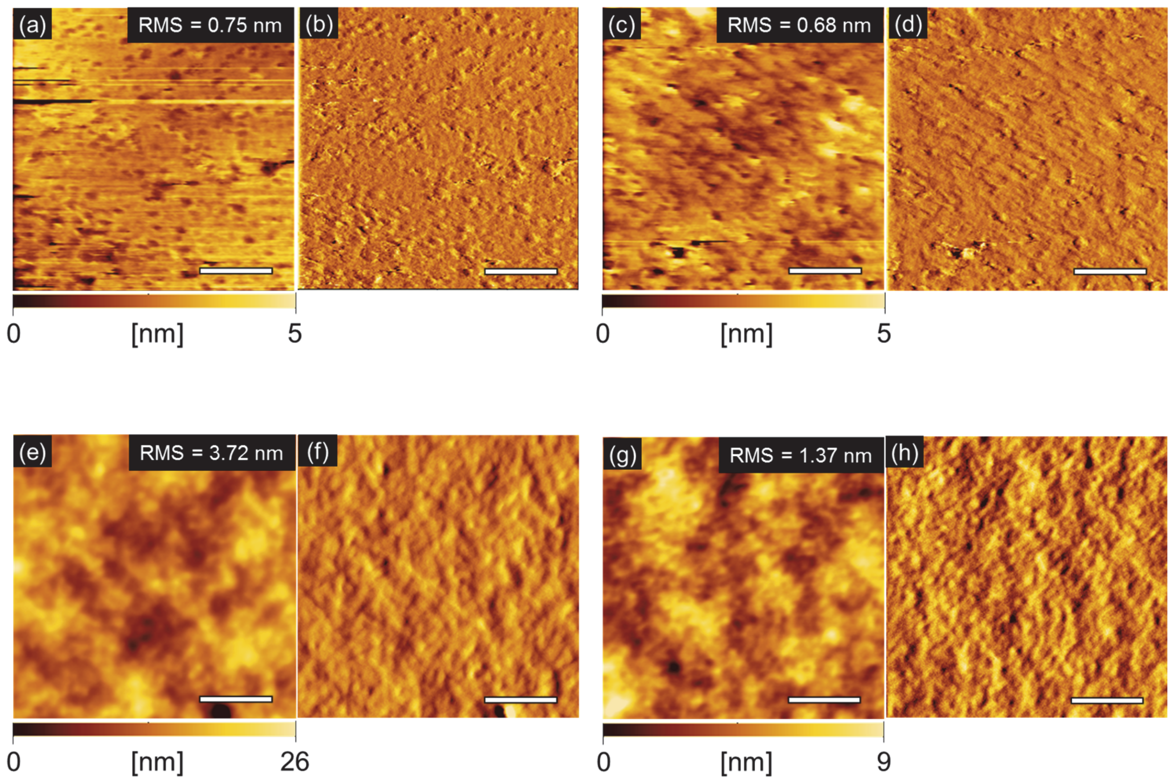

Figure S6. Topological (a,c,e,g) and error-signal (b,d,f,h) images (2 × 2 μm) of (a-d) **PATz4T-oR¹R²** films on FOTS-treated n^+-Si/SiO_2 substrate annealed at 250 °C, and (e-h) **PATz4T-oR¹R²**/$PC_{61}BM$ blended films on ITO/ZnO; (a,b,e,f) **PATz4T-o12HD**, and (c,d,g,h) **PATz4T-o6OD**. Blend ratios of polymer and $PC_{61}BM$ are 1:1 for **PATz4T-o12HD** and 1:2 for **PATz4T-o6OD**. The scale bar is 500 nm.

8. 1D Profiles and 2D Images of GIWAXS Measurement of PATz4T and blended films

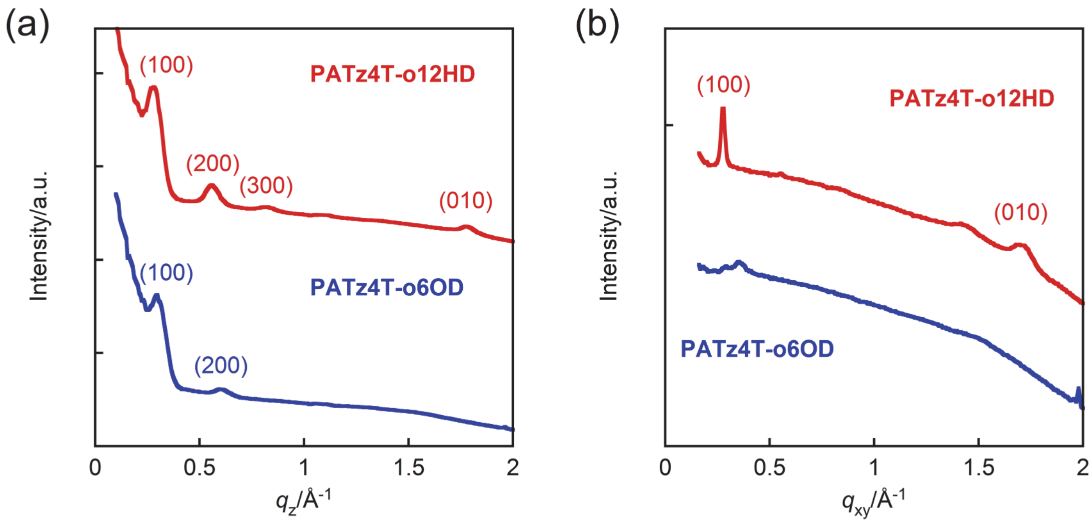

Figure S7. 1D profiles of GIWAXS images of **PATz4T** films annealed at 250 °C on FOTS-treated n^+-Si/SiO_2 substrate; (a) out-of-plane and (b) in-plane.

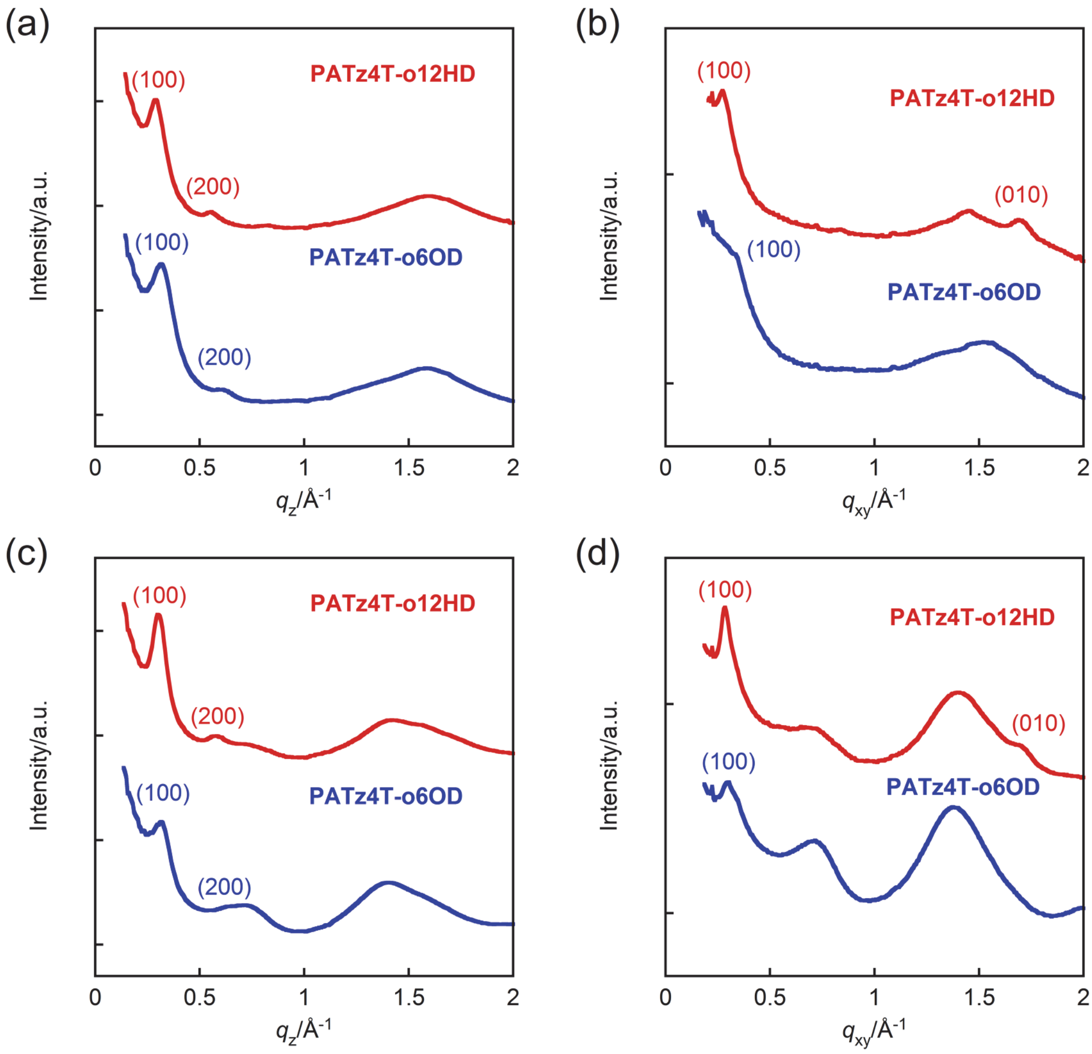

Figure S8. 1D profiles of GIWAXS images of pure **PATz4T** films (a,b) and blended films with $PC_{61}BM$ (c,d) on ZnO-coated ITO substrate; (a,c) out-of-plane and (b,d) in-plane. Blend ratios of polymer:$PC_{61}BM$ are 1:1 for **PATz4T-o12HD** and 1:2 for **PATz4T-o6OD**, respectively.

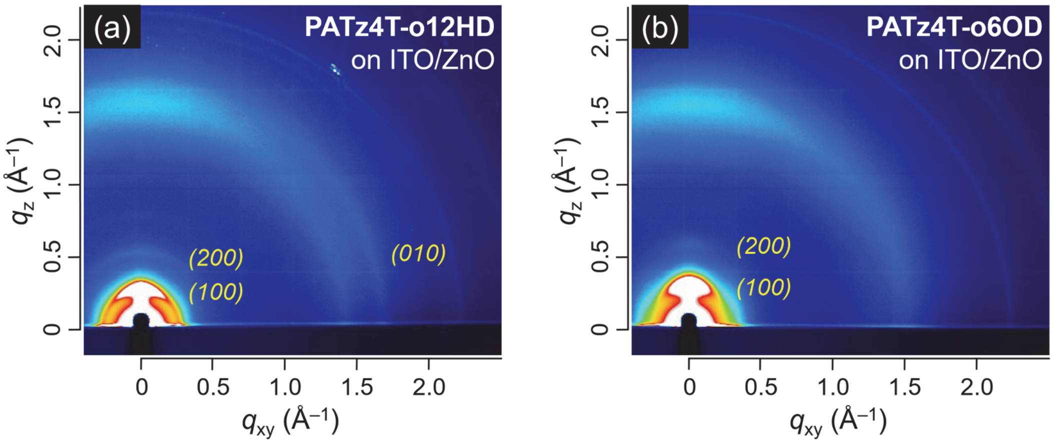

Figure S9. 2D GIWAXS images of pure **PATz4T** films on ZnO-coated ITO substrate; (a) **PATz4T-o12HD** and (b) **PATz4T-o6OD**.